International Refereed Journal of Engineering and Science (IRJES)
ISSN (Online) 2319-183X, (Print) 2319-1821
Volume 6, Issue 4 (April 2017), pp. 08-15

Buckling of a carbon nanotube embedded in elastic medium via nonlocal elasticity theory

A.M. Zenkour[1,2,*] and A.H. Banaji[1]

[1]*Department of Mathematics, Faculty of Science, King Abdulaziz University, P.O. Box 80203, Jeddah 21589, Saudi Arabia*
[2]*Department of Mathematics, Faculty of Science, Kafrelsheikh University, Kafrelsheikh 33516, Egypt*

Abstract:- Buckling analysis of a carbon nanotube (CNT) embedded in Pasternak's medium is investigated. Eringen's nonlocal elasticity theory in conjunction with the first-order Donell's shell theory is used. The governing equilibrium equations are obtained and solved for CNTs subjected to mechanical loads and embedded in Winkler-Pasternak's medium. Effects of nonlocal parameter, radius and length of CNT, as well as the foundation parameters on buckling of CNT are investigated. Comparison with the available results is made.

Keywords: nanotube; buckling; elastic foundation; Eringen's nonlocal elasticity.

I. INTRODUCTION

The carbon nanotubes (CNTs) embedded in elastic medium are the main subject of many investigators. It has been treated in most cases of buckling, bending and vibration analyses via a nonlocal elasticity theory. Eringen [1, 2] is firstly presented his theory of nonlocal elasticity to account for the scale effect in elasticity. He assumed that the stress at any point is treated as a functional of strains at all points in the solid. For this reason, the internal size scale could be considered in stress-strain constitutive equations simply as a material parameter of the solid.

The first-order shear deformation theory is considered as the basis of refined shell theories. It includes the effect of both transverse shear strain for bending and buckling problem and includes rotary inertia for the vibration problems. In fact, the Donnell and Sanders shear deformation theories [3, 4] are increasingly used to deal with the problem of cylindrical shell or micro- and nano-cylinders due to their simplicity and high accuracy. Many investigators have discussed the buckling of single-walled (SW) and multi-walled (MW) CNTs (Arani et al. [5] and Sudak [6]). Silvestre et al. [7] and Zhang et al. [8] proposed the buckling behavior of CNTs based on the Donnell-Sanders shell theory. Wang et al. [9] presented two nonlocal models for beam and shell to investigate the effect of small scale on the buckling analyses of CNTs. Ansari et al. [10] presented the axial buckling response of SWCNTs due to thermal environment effect. Ning et al. [11] investigated the dynamics and stability of a composed structure of outer cylindrical shell conveying swirling fluid in annulus between inner shell-type body and outer shell by travelling wave approach. Robinson and Adali [12] computed buckling loads for CNTs subjected to a combination of concentrated and axially distributed loads. Distributed axial loads are taken as uniformly distributed and triangularly distributed.

In most applications, the CNT is embedded in an elastic foundation medium. The first type of elastic foundation is presented by Winkler as a one-parameter elastic foundation (Murmu and Pradhan [13], Pradhan and Reddy [14], Narendar and Gopalakrishnan [15]). In fact, both the first type of elastic foundation and the second type presented by Pasternak should be employed to simulate the interaction of nanostructures with a surrounding elastic medium (Ghorbanpour Arani et al. [16], Mohammadi et al. [17] and Ansari et al. [18]).

This article presents the buckling response problem of a CNT embedded in Pasternak's medium based on the first-order shell theory. A comparison study with published results acquired by other investigators is presented showing an excellent agreement. The effects of different parameters on the range of validity and the buckling loads are investigated for CNTs embedded in an elastic medium.

II. BASIC EQUATIONS OF CARBON NANOTUBE (CNT)

2.1. Elastic medium

Consider a CNT of length L, radius R and thickness h as shown in Figure 1. The coordinate system of (x, θ, z) as x-axis is along the length of the CNT is introduced. The CNT is embedded in a Pasternak's medium. This foundation model is represented by

$$R_f = (K_1 - K_2\nabla^2)w(x, \theta, t), \tag{1}$$

*Professor, E-mail: zenkour@kau.edu.sa

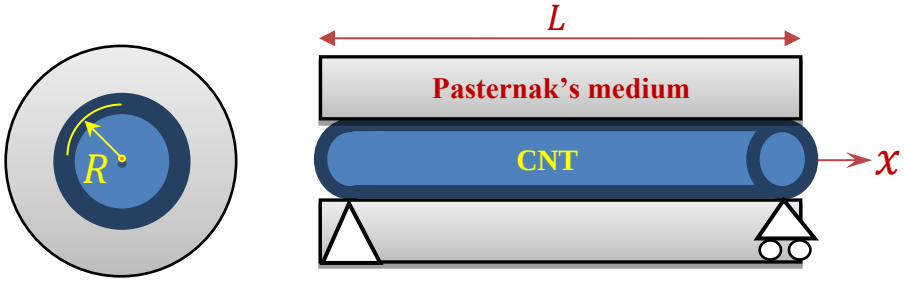

Fig. 1: Schematic diagram for simply-supported carbon nanotube embedded in Pasternak's foundations.

where w is the transverse displacement of CNT, K_1 represents Winkler's modulus and K_2 represents Pasternak's (shear) foundation modulus.

2.2. Nonlocal first-order theory

Based on the first-order shear deformation theory, the displacements of CNT can be expressed as

$$\begin{aligned} u_x(x,\theta,z,t) &= u(x,\theta,t) + z\,\varphi(x,\theta,t),\\ u_\theta(x,\theta,z,t) &= v(x,\theta,t) + z\,\psi(x,\theta,t),\\ u_z(x,\theta,z,t) &= w(x,\theta,t), \end{aligned} \tag{2}$$

where u and v are the reference in-plane surface displacements and φ and ψ represent the rotations. The Cauchy strain-displacement relations for normal strains ε_{xx} and $\varepsilon_{\theta\theta}$ and shear strains $\gamma_{x\theta}$, $\gamma_{\theta z}$ and γ_{xz} are given by

$$\varepsilon_{ij} = \varepsilon_{ij}^0 + z\varepsilon_{ij}^1, \tag{3}$$

where ε_{ij}^0 and ε_{ij}^1 are given by

$$\begin{aligned} &\varepsilon_{xx}^0 = \frac{\partial u}{\partial x}, \quad \varepsilon_{\theta\theta}^0 = \frac{1}{R}\frac{\partial v}{\partial \theta} + \frac{w}{R}, \quad \varepsilon_{x\theta}^0 = \frac{\partial v}{\partial x} + \frac{1}{R}\frac{\partial u}{\partial \theta}, \quad \varepsilon_{xz}^0 = \frac{\partial w}{\partial x} + \varphi,\\ &\varepsilon_{\theta z}^0 = \frac{1}{R}\frac{\partial w}{\partial \theta} - \frac{v}{R} + \psi, \quad \varepsilon_{xx}^1 = \frac{\partial \varphi}{\partial x}, \quad \varepsilon_{\theta\theta}^1 = \frac{1}{R}\frac{\partial \psi}{\partial \theta}, \quad \varepsilon_{x\theta}^1 = \frac{\partial \psi}{\partial x} + \frac{1}{R}\frac{\partial \varphi}{\partial \theta}. \end{aligned} \tag{4}$$

The constitutive relations are expressed as

$$\begin{aligned} \begin{Bmatrix} \sigma_{xx} - \xi^2\nabla^2\sigma_{xx} \\ \sigma_{\theta\theta} - \xi^2\nabla^2\sigma_{\theta\theta} \end{Bmatrix} &= \frac{E}{1-\nu^2}\begin{bmatrix} 1 & \nu \\ \nu & 1 \end{bmatrix}\begin{Bmatrix} \varepsilon_{xx} \\ \varepsilon_{\theta\theta} \end{Bmatrix},\\ \sigma_{ij} - \xi^2\nabla^2\sigma_{ij} &= G\varepsilon_{ij}, \quad i \neq j, \quad (i,j = x,\theta,z), \end{aligned} \tag{5}$$

in which $\xi = e_0 a$ represents the nonlocal parameter.

2.3. Equilibrium equations

The principle of virtual work is used for derivation of equilibrium equations on the basis of Donnell's shell theory as

$$\begin{aligned} &\frac{\partial N_{xx}}{\partial x} + \frac{1}{R}\frac{\partial N_{x\theta}}{\partial \theta} = 0, \quad \frac{\partial N_{x\theta}}{\partial x} + \frac{1}{R}\frac{\partial N_{\theta\theta}}{\partial \theta} + \frac{Q_\theta}{R} = 0,\\ &\frac{\partial Q_x}{\partial x} + \frac{1}{R}\frac{\partial Q_\theta}{\partial \theta} - \frac{N_{\theta\theta}}{R} + S_x\frac{\partial^2 w}{\partial x^2} + q - R_f = 0,\\ &\frac{\partial M_{xx}}{\partial x} + \frac{1}{R}\frac{\partial M_{x\theta}}{\partial \theta} - Q_x = 0, \quad \frac{\partial M_{x\theta}}{\partial x} + \frac{1}{R}\frac{\partial M_{\theta\theta}}{\partial \theta} - Q_\theta = 0, \end{aligned} \tag{6}$$

where q is the transverse load and S_x denotes membrane force caused by uniform axial compression. The quantities N_{ij}, M_{ij} and Q_i are the following nonlocal force and moment resultants:

$$\{N_{ij}, M_{ij}\} = \int_{-h/2}^{h/2}\{1, z\}\sigma_{ij}\mathrm{d}z, \quad Q_i = \int_{-h/2}^{h/2}\sigma_{iz}\mathrm{d}z. \tag{7}$$

With the aid of Eqs. (3)-(5), one gets the nonlocal resultants in the form

$$\begin{Bmatrix} N_{xx} - \xi^2\nabla^2 N_{xx} \\ N_{\theta\theta} - \xi^2\nabla^2 N_{\theta\theta} \\ N_{x\theta} - \xi^2\nabla^2 N_{x\theta} \end{Bmatrix} = \frac{Eh}{1-\nu^2}\begin{bmatrix} 1 & \nu & 0 \\ \nu & 1 & 0 \\ 0 & 0 & \frac{1-\nu}{2} \end{bmatrix}\begin{Bmatrix} \varepsilon_{xx}^0 \\ \varepsilon_{\theta\theta}^0 \\ \varepsilon_{x\theta}^0 \end{Bmatrix}, \tag{8}$$

$$\begin{Bmatrix} M_{xx} - \xi^2\nabla^2 M_{xx} \\ M_{\theta\theta} - \xi^2\nabla^2 M_{\theta\theta} \\ M_{x\theta} - \xi^2\nabla^2 M_{x\theta} \end{Bmatrix} = D\begin{bmatrix} 1 & \nu & 0 \\ \nu & 1 & 0 \\ 0 & 0 & \frac{1-\nu}{2} \end{bmatrix}\begin{Bmatrix} \varepsilon_{xx}^1 \\ \varepsilon_{\theta\theta}^1 \\ \varepsilon_{x\theta}^1 \end{Bmatrix}, \tag{9}$$

$$Q_x - \xi\nabla^2 Q_x = Gh\varepsilon_{xz}^0, \quad Q_\theta - \xi\nabla^2 Q_\theta = Gh\varepsilon_{\theta z}^0, \tag{10}$$

where $D = \frac{Eh^3}{12(1-\nu^2)}$ is the bending rigidity of the CNT, E is Young's modulus and ν is Poisson's ratio. So, the equilibrium equations of the present CNT embedded in a Pasternak's medium are finalized as

$$\begin{aligned}
&\frac{Eh}{1-\nu^2}\frac{\partial^2 u}{\partial x^2} + \frac{Gh}{R^2}\frac{\partial^2 u}{\partial \theta^2} + \frac{(2-\nu)Eh}{R(1-\nu^2)}\frac{\partial^2 v}{\partial x\partial\theta} + \frac{\nu Eh}{R(1-\nu^2)}\frac{\partial w}{\partial x} = 0,\\
&\frac{(2-\nu)Eh}{R(1-\nu^2)}\frac{\partial^2 u}{\partial x\partial\theta} + \frac{Eh}{2(1+\nu)}\frac{\partial^2 v}{\partial x^2} + \frac{Eh}{R^2(1-\nu^2)}\frac{\partial^2 v}{\partial\theta^2} + \frac{(3-2\nu)Eh}{R^2(1-\nu^2)}\frac{\partial w}{\partial\theta} - \frac{Gh}{R^2}v + \frac{Gh}{R}\psi = 0,\\
&-\frac{\nu Eh}{R(1-\nu^2)}\frac{\partial u}{\partial x} - \frac{(3-2\nu)Eh}{R^2(1-\nu^2)}\frac{\partial v}{\partial\theta} - Gh\left(\frac{\partial^2 w}{\partial x^2} + \frac{1}{R^2}\frac{\partial^2 w}{\partial\theta^2}\right) - \frac{Eh}{R^2(1-\nu^2)}w + Gh\frac{\partial\varphi_x}{\partial x} + \frac{Gh}{R}\frac{\partial\psi}{\partial\theta}\\
&+S_x\left[\frac{\partial^2 w}{\partial x^2} - \xi\left(\frac{\partial^4 w}{\partial x^4} + \frac{1}{R^2}\frac{\partial^4 w}{\partial x^2\partial\theta^2}\right)\right] + q - \left[K_1 - K_2\left(\frac{\partial^2}{\partial x^2} + \frac{1}{R^2}\frac{\partial^2}{\partial\theta^2}\right)\right]w - \xi\left(\frac{\partial^2 q}{\partial x^2} + \frac{1}{R^2}\frac{\partial^2 q}{\partial\theta^2}\right)\\
&+K_1\xi\left(\frac{\partial^2 w}{\partial x^2} + \frac{1}{R^2}\frac{\partial^2 w}{\partial\theta^2}\right) - K_2\xi\left(\frac{\partial^4 w}{\partial x^4} + \frac{2}{R^2}\frac{\partial^4 w}{\partial x^2\partial\theta^2} + \frac{1}{R^4}\frac{\partial^4 w}{\partial\theta^4}\right) = 0,\\
&-Gh\frac{\partial w}{\partial x} + D\left(\frac{\partial^2\varphi_x}{\partial x^2} + \frac{1-\nu}{2R^2}\frac{\partial^2\varphi_x}{\partial\theta^2}\right) + \frac{(1+\nu)D}{2R}\frac{\partial^2\psi}{\partial x\partial\theta} - Gh\varphi_x = 0,\\
&\frac{Gh}{R}v - \frac{Gh}{R}\frac{\partial w}{\partial\theta} + \frac{(1+\nu)D}{2R}\frac{\partial^2\varphi_x}{\partial x\partial\theta} + D\left(\frac{1-\nu}{2}\frac{\partial^2\psi}{\partial x^2} + \frac{1}{R^2}\frac{\partial^2\psi}{\partial\theta^2}\right) - Gh\psi = 0.
\end{aligned} \tag{11}$$

III. SOLUTION OF THE PROBLEM

For a simply-supported CNT the displacements and rotations may be assumed by

$$\begin{Bmatrix}\{u,\varphi\}\\ w\\ \{v,\psi\}\end{Bmatrix} = \begin{Bmatrix}\{hU_{mn},\Phi_{mn}\}\cos(\lambda x)\cos(n\theta)\\ hW_{mn}\sin(\lambda x)\cos(n\theta)\\ \{hV_{mn},\Psi_{mn}\}\sin(\lambda x)\sin(n\theta)\end{Bmatrix}, \tag{12}$$

where U_{mn}, V_{mn}, W_{mn}, Φ_{mn} and Ψ_{mn} are arbitrary constant parameters; n is the circumferential wave number and $\lambda = m\pi/L$ in which m is the axial wave number.

In what follows the following dimensionless variables will be used,

$$\xi = \frac{\xi^2}{L^2}, \quad \bar{S}_x = \frac{h}{EL^2}S_x, \quad \{\bar{K}_1,\bar{K}_2\} = \frac{h}{E}\left\{K_1,\frac{K_2}{L^2}\right\}. \tag{13}$$

Then, the governing equations given in Eq. (11), after using Eq. (12) and the above dimensionless form become

$$([C] - \bar{S}_x[P])\{\Delta\} = 0, \tag{14}$$

where $\{\Delta\} = \{U_{mn}, V_{mn}, W_{mn}, \Phi_{mn}, \Psi_{mn}\}^{\mathrm{T}}$ is the solution vector. The non-vanishing elements of the symmetric matrix $[C]$ are expressed as:

$$\begin{aligned}
&C_{11} = -\frac{\mathcal{M}_2}{2(1-\nu^2)}\left(\frac{h}{L}\right)^2, \quad C_{12} = \frac{mn\pi}{2(1-\nu)}\frac{h}{L}\frac{h}{R}, \quad C_{13} = \frac{\nu m\pi}{1-\nu^2}\frac{h}{L}\frac{h}{R},\\
&C_{22} = -\frac{\mathcal{M}_3}{2(1-\nu^2)}\left(\frac{h}{L}\right)^2 - \frac{1}{2(1+\nu)}\left(\frac{h}{R}\right)^2, \quad C_{23} = -\frac{(3-\nu)n}{2(1-\nu^2)}\left(\frac{h}{R}\right)^2, \quad C_{25} = \frac{1}{2(1+\nu)}\frac{h}{R},\\
&C_{33} = -\frac{\mathcal{M}_1}{2(1+\nu)}\left(\frac{h}{L}\right)^2 - \frac{1}{1-\nu^2}\left(\frac{h}{R}\right)^2 - \left(1+\xi\mathcal{M}_1\right)(\bar{K}_1 + \bar{K}_2\mathcal{M}_1), \quad C_{34} = -\frac{m\pi}{2(1+\nu)}\frac{h}{L},\\
&C_{35} = nC_{25}, \quad C_{44} = \frac{1}{12}C_{11} - \frac{1}{2(1+\nu)}, \quad C_{45} = \frac{1}{12}C_{12},\\
&C_{55} = -\frac{\mathcal{M}_3}{24(1-\nu^2)}\left(\frac{h}{L}\right)^2 - \frac{1}{2(1+\nu)},
\end{aligned} \tag{15}$$

where

$$\{\mathcal{M}_1,\mathcal{M}_2,\mathcal{M}_3\} = \{1,2,1-\nu\}m^2\pi^2 + \{1,1-\nu,2\}n^2\left(\frac{L}{R}\right)^2. \tag{16}$$

Also, the non-vanishing element of the matrices $[P]$ is expressed as

$$P_{33} = m^2\pi^2\left(\frac{L}{R}\right)^4\left(1+\mathcal{M}_1\xi\right). \tag{17}$$

The buckling parameter is given form Eq. (14) by setting the determinant $([C] - \bar{S}_x[P])$ equals zero.

IV. NUMERICAL RESULTS AND DISCUSSIONS

4.1 Validation

The effects of nonlocal parameter (ξ), length (L), radius (R), Winkler-Pasternak's foundation (K_1, K_2) and mode numbers (m, n) on the buckling analysis of the CNTs will be presented. Tables 1 and 2 show how the

present results can be validated by other published literatures in buckling analysis of CNTs at different wave numbers in longitudinal and circumferential directions (Wang et al. [9] and Ansari et al. [10]).

The ratio of nonlocal axial buckling load to the local axial buckling load is defined as

$$\beta_r = \frac{S_x^{NL}}{S_x^L}. \tag{18}$$

The material properties for the present CNT are accepted as

$$E = 1\ \text{TPa}, \quad \nu = 0.3, \quad \alpha = 1.1 \times 10^{-6}\ 1/\text{K}. \tag{19}$$

Table 1 Comparison of axial buckling load ratio β_r of the CNT at lower wave modes in longitudinal and circumferential directions.

m	Reference	n			
		1	2	3	4
1	[10]	0.057488	0.01529174	0.006877826	0.003885
	Present	0.05748849	0.0152917397	0.0068778258	0.00388508
2	[10]	0.053824	0.015019720	0.006822253	0.003867
	Present	0.05382381	0.0150197201	0.0068222533	0.00386729
3	[10]	0.048655	0.014587241	0.006731601	0.003838
	Present	0.04865456	0.0145872414	0.0067316016	0.00383799
4	[10]	0.042888	0.014021991	0.006608663	0.003798
	Present	0.04288799	0.0140219913	0.0066086636	0.00379771

Table 2 Comparison of axial buckling load ratio β_r of the CNT at higher wave modes in longitudinal and circumferential directions.

m	Reference	n				
		0	1	2	3	4
5	[9]	0.091999809	0.037217	0.013356558	0.006457046	0.003747
	Present	0.091999668	0.03721677	0.0133565552	0.0064570449	0.00374715
6	[9]	0.065736684	0.032039	0.012624317	0.006280925	0.003687
	Present	0.065736580	0.03203872	0.0126243131	0.0062809245	0.00368715
7	[9]	0.049153595	0.027515	0.011856153	0.006084783	0.003619
	Present	0.049153516	0.02751454	0.0118561482	0.0060847820	0.00361867

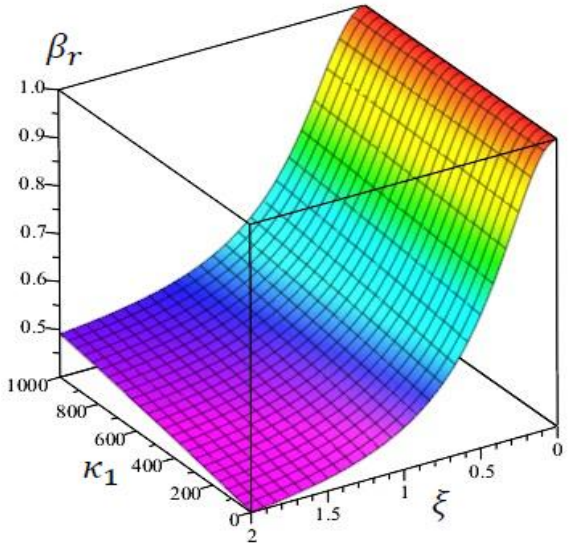

Fig. 2: Variation of buckling ratio β_r with nonlocal parameter ξ and Winkler's foundation κ_1.

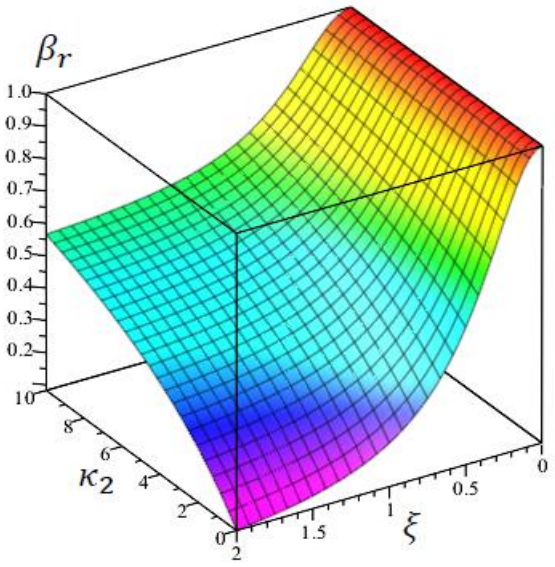

Fig. 3: Variation of buckling ratio β_r with nonlocal parameter ξ and Pasternak's foundation κ_2.

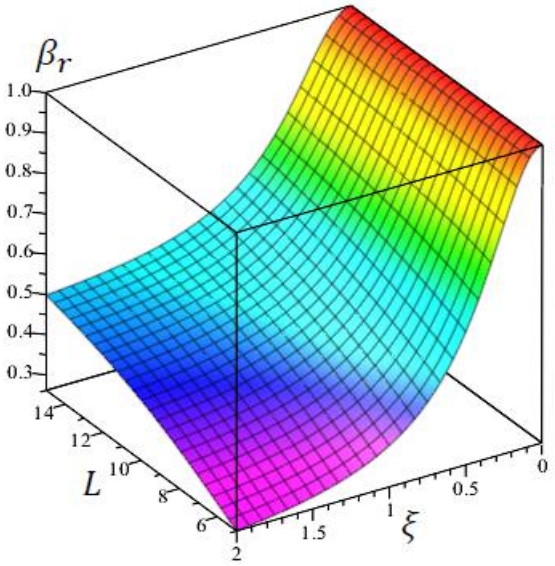

Fig. 4: Variation of buckling ratio β_r with nonlocal parameter ξ and length L of the CNT.

The CNT is of radius $R = 0.5$ nm, length $L = 10$ nm, and thickness $h = 0.34$ nm. In addition, the nonlocal value is taken as $\xi = 2$ nm^2.

Table 1 shows a comparison of axial buckling load ratio β_r of the CNT subjected to axial buckling load calculated by using the present theory with those obtained by Ansari et al. [10]. It is clear that there is excellent agreement between the present results and those reported in [10]. This excellent agreement achieved clarifies the capability of method used in predicting nonlocal critical buckling loads of CNTs. The buckling ratio is decreasing with the increase of the wave modes.

Table 2 shows a comparison study of axial buckling load ratio β_r of the CNT subjected to axial buckling load calculated by using the present theory with those obtained by Wang et al. [9]. Once again there is excellent agreement between the present results and those in [9]. The effect of small scale becomes more pronounced for shorter wavelength at higher buckling modes.

4.2 Benchmark buckling load ratio

Now, it is interesting to investigate the influence of elastic foundation parameters on the axial buckling load ratio β_r of the CNT. It is assumed that the dimensionless foundation parameters of Pasternak's model are given as

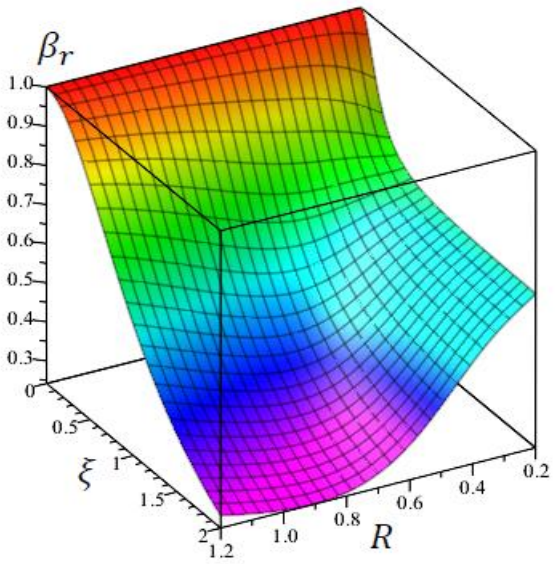

Fig. 5: Variation of buckling ratio β_r with nonlocal parameter ξ and radius R of the CNT.

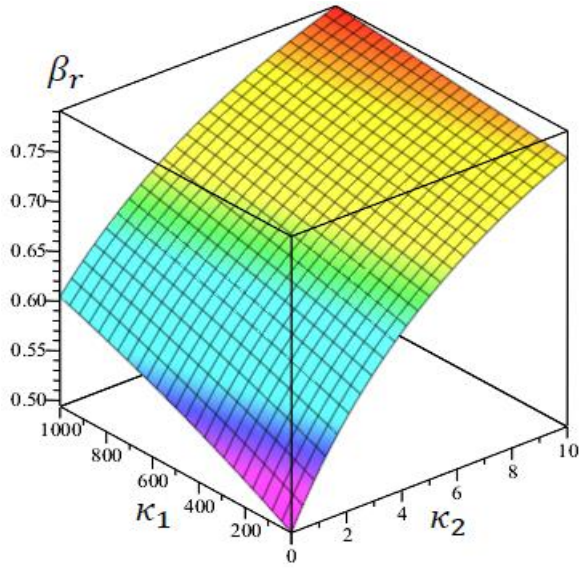

Fig. 6: Variation of buckling ratio β_r with Winkler-Pasternak's foundations κ_1 and κ_2.

$$\kappa_1 = \frac{L^4 K_1}{D}, \quad \kappa_2 = \frac{L^2 K_2}{D}. \tag{20}$$

Figures 2-8 show the two-dimensional variation of β_r versus nonlocal parameter ξ, length L, radius R, and the foundation parameters κ_1 and κ_2. It is assumed, except otherwise stated, that $m = n = 1$, $\xi = 0.5$ nm^2, $R = 0.5$ nm, $L = 10$ nm, $h = 0.34$ nm, $\kappa_1 = 100$ nN, and $\kappa_2 = 5$ nN.

Figure 2 illustrates the variation of buckling ratio β_r with the two-dimensional variation of nonlocal parameter ξ and Winkler's foundation κ_1. The buckling load ratio β_r is rabidly decreasing as ξ increases and β_r is slowly increasing as κ_1 increases. The Winkler's parameter has no effect on β_r when $\xi = 0$ (the local case). The minimum value of β_r occurs when $\xi = 0.2$ and $\kappa_1 = 0$.

Figure 3 shows the variation of buckling load ratio β_r with the two-dimensional variation of nonlocal parameter ξ and Pasternak's foundation κ_2. Once again, the buckling load ratio β_r is rabidly decreasing as ξ increases and increasing as κ_2 increases. The Pasternak's parameter has no effect on β_r when $\xi = 0$ (the local case). The minimum value of β_r occurs when $\xi = 0.2$ and $\kappa_2 = 0$.

Figure 4 shows the variation of buckling load ratio β_r with the two-dimensional variation of nonlocal parameter ξ and length L of the CNT. The buckling load ratio β_r is rabidly decreasing as ξ increases and increasing as L increases. The minimum value of β_r occurs at higher values of ξ and small value of L.

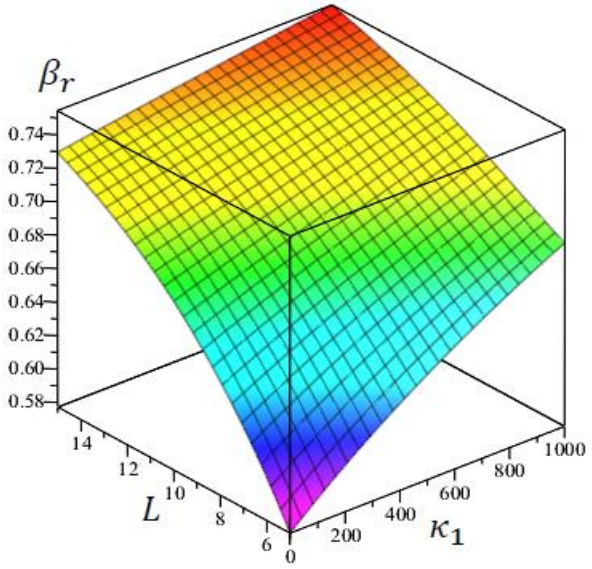

Fig. 7: Variation of buckling ratio β_r with Winkler's foundation κ_1 and Length L of the CNT.

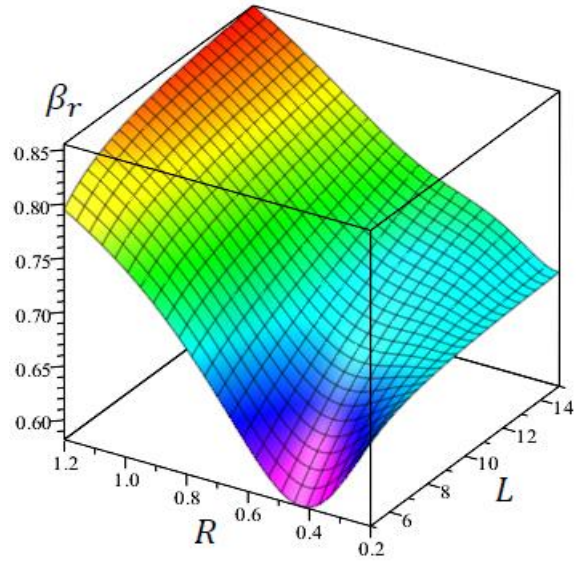

Fig. 8: Variation of buckling ratio β_r with the dimensions L and R of the CNT.

Figure 5 illustrates the variation of buckling ratio β_r with the two-dimensional variation of nonlocal parameter ξ and radius R of the CNT. The buckling load ratio β_r is rabidly decreasing as ξ increases. Also, β_r is no longer decreasing and has its minimum at $R = 0.9$ for higher values of ξ. The maximum value of β_r occurs when $\xi = 0$ (the local case) and this irrespective of the value of R.

Figure 6 shows the variation of buckling load ratio β_r with the two-dimensional variation of Winkler-Pasternak's foundation κ_1 and κ_2. The buckling load ratio β_r is rabidly increasing as κ_2 increases and increasing as κ_1 increases. The Pasternak's parameter has no effect on β_r when $\xi = 0$ (the local case). The minimum value of β_r occurs in the case of without elastic foundations and the maximum occurs for the higher values of κ_1 and κ_2. The buckling load ratio β_r is sensitive to the value of κ_2 more than the value of κ_1.

Figure 7 illustrates the variation of buckling ratio β_r with the two-dimensional variation of Winkler's foundation κ_1 and the length L of the CNT. The buckling load ratio β_r is rabidly increasing as L increases and β_r is slowly increasing as κ_1 increases. The minimum value of β_r occurs when $L = 0.5$ and $\kappa_1 = 0$. The maximum value of β_r occurs at higher values of L and κ_1.

Finally, Figure 8 illustrates the variation of buckling ratio β_r versus the dimensions L and R of the CNT. The buckling load ratio β_r is slowly increasing as L increases. Also, β_r is no longer decreasing as R increases and

has a minimum value at $R = 0.44$ for higher values of L. The maximum value of β_r occurs at higher values of L and R.

V. CONCLUSIONS

The paper presents a carbon nanotube that embedded in Winkler-Pasternak's foundation medium. The buckling analysis is obtained by using Eringen's nonlocal elasticity theory and the first-order shell theory. A validation example is given to show the accuracy of the present analysis. The obtained numerical results show that:

- The buckling load ratio β_r is rabidly decreasing as the nonlocal parameter ξ increases.
- The maximum value of β_r occurs for the local case and this irrespective of the values of other parameters.
- The minimum value of β_r occurs in the case of without elastic foundations and the maximum one occurs for the higher values of the foundation parameters κ_1 and κ_2.
- The foundation parameters κ_1 and κ_2 have no effect on β_r when $\xi = 0$ (the local case).
- The buckling load ratio β_r is sensitive to the value of Pasternak's parameter κ_2 more than the value of Winkler's parameter κ_1.
- The buckling load ratio β_r is increasing as the length L of the CNT increases.
- The maximum value of β_r occurs at higher values of the dimensions L and R of the CNT.

REFERENCES

[1] A.C. Eringen, Nonlocal polar elastic continua, *Int J Eng Sci*, 10, 1–16, 1972.

[2] A.C. Eringen, On differential equations of nonlocal elasticity and solutions of screw dislocation and surface waves, *J Appl Phys* 54, 4703–4710, 1983.

[3] L.H. Donnell, A new theory for the buckling of thin cylinders under axial compression and bending, *Trans ASME* 56, 795–806, 1934.

[4] J.L. Sanders, *An Improved First Approximation Theory for Thin Shells*, NASA TR-R24 (1959).

[5] A. Ghorbanpour Arani, R. Rahmani, A. Arefmanesh, Elastic buckling analysis of single-walled carbon nanotube under combined loading by using the ANSYS software, *Phys E* 40, 2390–2395, 2008.

[6] L.J. Sudak, Column buckling of multiwalled carbon nanotubes using nonlocal continuum mechanics, *J Appl Phys* 94, 7281, 2003.

[7] N. Silvestre, C.M. Wang, Y.Y. Zhang, Y. Xiang, Sanders shell model for buckling of single-walled carbon nanotubes with small aspect ratio, *Compos Struct* 93, 1683–1691, 2011.

[8] Y.Q. Zhang, G.R. Liu, J.S. Wang, Small-scale effects on buckling of multiwalled carbon nanotubes under axial compression, *Phys Rev B* 70, 205430, 2004.

[9] Q. Wang, V.K. Varadan, S.T. Quek, Small scale effect on elastic buckling of carbon nanotubes with nonlocal continuum models, *Phys Letters A* 357, 130–135, 2006.

[10] R. Ansari, S. Sahmani, H. Rouhi, Axial buckling analysis of single-walled carbon nanotubes in thermal environments via the Rayleigh–Ritz technique, *Comput Mater Sci* 50, 3050–3055, 2011.

[11] W.B. Ning, D.Z. Wang, J.G. Zhang, Dynamics and stability of a cylindrical shell subjected to annular flow including temperature effects, *Arch Appl Mech*, 86, 643–656, 2016.

[12] M.T.A. Robinson, S. Adali, Variational solution for buckling of nonlocal carbon nanotubes under uniformly and triangularly distributed axial loads, *Compos Struct* 156, 101–107, 2016.

[13] T. Murmu, S.C. Pradhan, Thermal effects on the stability of embedded carbon nanotubes, *Comput Mater Sci* 47, 721–726, 2010.

[14] S.C. Pradhan, G.K. Reddy, Buckling analysis of single walled carbon nanotube on Winkler foundation using nonlocal elasticity theory and DTM, *Comput Mater Sci* 50, 1052–1056, 2011.

[15] S. Narendar, S. Gopalakrishnan, Critical buckling temperature of single-walled carbon nanotubes embedded in a one-parameter elastic medium based on nonlocal continuum mechanics, *Phys E* 43, 1185–1191, 2011.

[16] A. GhorbanpourArani, M.S. Zarei, M. Mohammadimehr, A. Arefmanesh, M.R. Mozdianfard, The thermal effect on buckling analysis of a DWCNT embedded on the Pasternak foundation, *Phys E* 43, 1642–1648, 2011.

[17] M. Mohammadi, A. Farajpour, A. Moradi, M. Ghayour, Shear buckling of orthotropic rectangular graphene sheet embedded in an elastic medium in thermal environment, *Compos B* 56, 629–637, 2014.

[18] R. Ansari, R. Gholami, S. Sahmani, A. Norouzzadeh, and M. Bazdid-Vahda, Dynamic stability analysis of embedded multi-walled carbon nanotubes in thermal environment, *Acta Mech Solida Sin* 28, 659–667, 2015.